

Break-up, coalescence and self-guiding of femtosecond laser pulses in air

A. Couairon, L. Bergé,

*Commissariat à l'Énergie Atomique, Bruyères-le-Châtel, B.P. 12,
91680 Bruyères-le-Châtel, France
couairon@bruyeres cea.fr, berge@bruyeres cea.fr*

S. Tzortzakis, M. Franco, A. Chiron, B. Lamouroux,
Y-B. André, B. Prade, and A. Mysyrowicz

*Laboratoire d'Optique Appliquée, CNRS UMR 7639, École Nationale Supérieure
des Techniques Avancées - École Polytechnique, Chemin de la Lumière,
F-91761 Palaiseau Cedex, France
stzortz@ensta.ensta.fr, mysy@ensta.ensta.fr*

Abstract: Femtosecond laser pulses propagating in air are investigated. For input powers as high as 25 times the self-focusing threshold, the pulses are shown to break up into two spots, which coalesce into a self-guided beam.

© 2000 Optical Society of America

OCIS codes: 190.5530 Pulse propagation and Solitons, 320.7110 Ultrafast nonlinear optics

1 Introduction

Nowadays, there is a considerable interest in understanding the propagation of femtosecond laser pulses through the atmosphere. Self-guided infra-red (IR) laser beams with high peak power forming an intense filament over long distances have indeed been reported by several groups [1, 2, 3]. On the other hand, various attempts in modeling this phenomenon have been proposed, either by solving numerically nonlinear Schrödinger like systems or by using more analytical approaches [4, 5, 6, 7]. Although there is a wide consensus on the physical effects sustaining this unusual propagation, controversies still remain about the detailed dynamics of the pulse during the early stage in the self-guiding mechanism [5]. In particular, high-power pulses have been observed to undergo modulational instability producing multiple filaments, before relaxing to one or two waveguides [3]. The role of this filamentation stage in the evolution of ultra-short pulses is, however, still unclear.

In this contribution, we study the propagation of femtosecond IR pulses exhibiting a single transverse mode within a well-defined geometry, with pulse peak powers above critical. Emphasis is laid on two specific points: First, we examine the global features in the wave propagation and underline its three characteristic stages, namely: (i) the self-focusing of the pulse in Kerr regime, (ii) the generation of an electron plasma by multiphoton ionization, and (iii) the formation of a self-guided beam by coupling between the electron plasma and the intense beam. These data, collected experimentally, are compared with results from an axis-symmetric numerical code, which involves the main ingredients for describing the propagation of ultra-short pulses in air. Second, we detail the early propagation of high-power beams: For different input energies and powers, we investigate, both experimentally and theoretically, the break-up of perturbed Gaussianlike pulses and display evidence of their ability to recombine for producing a self-guided structure.

2 Experimental procedure and numerical modeling

The laser source is a Ti:Sapphire oscillator-amplifier operating at kHz rate and at the wavelength $\lambda_0 = 800$ nm. It delivers pulses of 40 fs duration with an energy of up to 8 mJ per pulse. The pulse time profile is measured accurately by cross-phase modulation or by the SPIDER technique. The pulse diameter is first reduced by an inverted telescope and then launched through the atmosphere in the form of a converging beam with focal distances varying from $f = 2$ m to infinity. The following measurements are performed as a

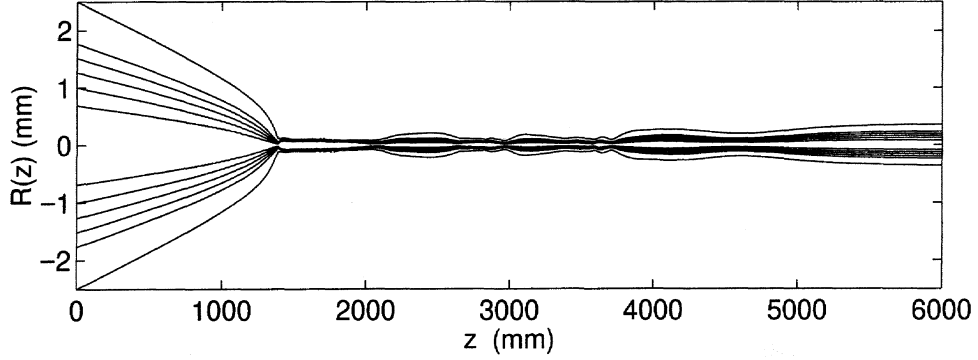


Fig. 1. Beam radius of a self-guided filament focused by a lens of focal length $f = +2$ m, with input energy $E_{in} = 3.4$ mJ. The electron plasma fully develops from $z \geq 1.3$ m.

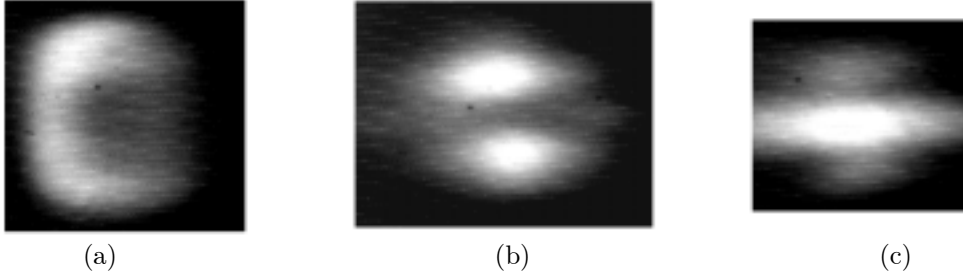


Fig. 2. Input beam (5 mJ) propagating freely in air ($f = +\infty$). (a) Ring structure, $z = 250$ cm. (b) Two-spot formation, $z = 650$ cm, (c) Coalescence into a self-guided filament, $z = 850$ cm.

function of the propagation distance for different incident pulse powers: beam diameter, energy and spectrum of the self-guided pulse, and the electron density resulting from air ionization.

A detailed numerical analysis of the same pulses is developed from a three-dimensional code with axial symmetry. This code encompasses the effects of diffraction, the nonlinear optical Kerr response of the medium, with both instantaneous and retarded components in a ratio $\frac{1}{2}$ fixed by experimental evidence, together with the air ionization by multiphoton transitions. It resolves the slowly-varying envelope of the laser electric field $\mathcal{E}(r, z, t)$, which is governed by the nonlinear Schrödinger equation

$$2i \frac{\partial \mathcal{E}}{\partial z} + \frac{1}{k_0} \Delta_{\perp} \mathcal{E} - k'' \frac{\partial^2 \mathcal{E}}{\partial t^2} + k_0 n_2 \{ |\mathcal{E}|^2 + \int_{-\infty}^t e^{-(t-t')/\tau_K} |\mathcal{E}(t')|^2 dt' \} \mathcal{E} - k_0 \frac{\omega_{pe}^2(\rho)}{\omega_0^2} \mathcal{E} + i\beta^{(K)} |\mathcal{E}|^{2K-2} \mathcal{E} = 0, \quad (1)$$

coupled with the density ρ of the electron plasma created by ionization. This quantity evolves as

$$\frac{\partial \rho}{\partial t} = \sigma |\mathcal{E}|^{2K} (\rho_{at} - \rho), \quad (2)$$

where $\rho_{at} = 2.7 \times 10^{19} \text{ cm}^{-3}$ is the density of neutral atoms. The input pulses exhibit transverse waists fixed at about $w_0 = 3$ mm, and they are either collimated, or focused by a lens with focal length $f = 2$ m. At atmospheric pressure, the appropriate parameters are $n_2 = 3.2 \times 10^{-19} \text{ cm}^2/\text{W}$, $K = 10$, $\tau_p = 70$ fs, $\beta^{(10)} \sim 10^{-126} \text{ cm}^{17}/\text{W}^9$, $\sigma \simeq 2 \times 10^{-128} \text{ cm}^{20} \text{ W}^{-10} \text{ s}^{-1}$ and the critical power for self-focusing is $P_{cr} \simeq 3.5$ GW.

3 Results

- Global dynamics of light self-guiding

A self-guided filament is observed to form when the input power is above the critical power for self-focusing, P_{cr} . In this situation, the wave grows up, excites an electron plasma by ionization, from which a steady-state filament results. This point has been detailed for incident pulses being narrow in space [$w_0 = 3$ mm, Fig. 1] and having an input energy increased from $E_{\text{in}} = 1$ mJ to $E_{\text{in}} = 5$ mJ, which corresponds to input powers belonging to the range $6 \leq P_{\text{in}}/P_{\text{cr}} \leq 30$. The numerical results show that, for these powers and with a lens $f = 2$ m, the pulse forms a self-focused beam, creates an electron plasma and then forms a robust filament, which is able to propagate over several Rayleigh lengths $z_f = z_0 f^2 / (z_0^2 + f^2) \sim 11.3$ cm, where $z_0 \sim 35$ m is the diffraction length of the collimated beam. As shown by Fig. 1, these three stages recalled above are clearly depicted by our numerical code for Gaussian input beams, whose spatial shape is controlled and exhibits no perturbation.

- Filamentation at high power levels

From the experimental data, the propagation of femtosecond pulses in air is well described by the previous stages of nonlinear focusing followed by the formation of a waveguide structure at low energy levels only (i.e., for input powers below $10 P_{\text{cr}}$). For instance, a pulse with weak energy $E_{\text{in}} = 1$ mJ reproduces qualitatively the same features as above. In contrast, for input energies exceeding 2 mJ and containing powers above $10 P_{\text{cr}}$, the pulse undergoes Kerr filamentation triggered by the local inhomogeneities that degrade the quality of the beam : The pulse first forms a spatial ring [Fig. 2(a)], which in turn breaks up into two symmetric spots due to the usual modulational instability in Kerr media [Fig. 2(b)]. At later propagation distances, the two spots coalesce and reform the pulse into one central lobe [Fig. 2(c)]. These results are generic, even when the beam is focused by a lens. For explaining this mechanism, we derive some analytical estimates of filamentation growth rate, typical modulation length and coalescence criteria from standard arguments of modulation instability theory applied to a simplified nonlinear Schrödinger model. These estimates are shown to support the comparison with the experimental observations. Furthermore, the annular break-up and the underlying dynamics governing the interaction between filamentary structures are shown to be in qualitative agreement with similar results displayed by the numerical code, when the experimental profiles are used.

References

1. A. Braun, G. Korn, X. Liu, D. Du, J. Squier and G. Mourou, *Opt. Lett.* **20**, 73 (1995).
2. E.T.J. Nibbering, P.F. Curley, G. Grillon, B.S. Prade, M.A. Franco, F. Salin, and A. Mysyrowicz, *Opt. Lett.* **21**, 62 (1996).
3. B. La Fontaine, F. Vidal, Z. Jiang, C. Y. Chien, D. Comtois, A. Desparois, T.W. Johnston, J.-C. Kieffer, H. Pépin, and H.P. Mercure, *Phys. Plasmas* **6**, 1615 (1999).
4. M. Mlejnek, E.M. Wright and J.V. Moloney, *Opt. Lett.* **23**, 5 (1998).
5. M. Mlejnek, M. Kolesik, J.V. Moloney and E.M. Wright, *Phys. Rev. Lett.* **83**, 2938 (1999).
6. A. Chiron, B. Lamouroux, R. Lange, J.-F. Ripoche, M. Franco, B. Prade, G. Bonnaud, G. Riazuelo, and A. Mysyrowicz, *Eur. Phys. J. D* **6**, 383 (1999).
7. A. Couairon and L. Bergé, *Phys. Plasmas* **7**, 193 (2000); L. Bergé and A. Couairon, *Phys. Plasmas* **7**, 210 (2000).